Deep-Sea Research, Vol. 36, No. 11, pp. 1607–1620, 1989.
Printed in Great Britain.

0198–0149/89 $3.00 + 0.00

Isopycnal mixing and the distribution of particles across the North Pacific Subtropical Front

LIBE WASHBURN,* DAVID A. SIEGEL,*† TOMMY D. DICKEY*
and MICHAEL K. HAMILTON*

(*Received* 15 *June* 1988; *in revised form* 30 *April* 1989; *accepted* 26 *June* 1989)

Abstract—Vertical profiles of salinity S and beam attenuation coefficient c were obtained from the research platform R.P. *Flip* as it drifted across the North Pacific Subtropical Front (NPSF) during the Optical Dynamics Experiment (ODEX) in the autumn of 1982. Near-surface waters north of the NPSF have lower S and generally higher values of c compared with waters to the south. An anomaly in c is used to show that mixing and interleaving of S and c between these water masses extends to a depth of about 200 m. This activity results in the production of fine structure in S and c on vertical scales from a few meters to tens of meters. Isopycnal time series of S and c often are highly correlated on a 2 day time scale, which corresponds to spatial scales of order 10–30 km. High correlation is most frequently observed below the 1% light level and is consistent with conservative scalar-like behavior of c. The observed correlation indicates that isopycnal mixing and advection processes are important in controlling particle distributions, and thus c, in the vicinity of the NPSF.

1. INTRODUCTION

AN important optical parameter that has proven useful in characterizing various water masses is the beam attenuation coefficient c (cf. JERLOV, 1976). SPINRAD (1986) has developed theoretical calibration curves that relate c to the suspended particle volume V or $c = \alpha V$, where α depends upon the relative refractive index of the particles and the slope of an assumed hyperbolic particle-size distribution. A consequence of this relationship is that variations in c are proportional to changes in the concentration of suspended particles. Further discussions on the relationship between c and particle concentration under various conditions are given by JERLOV (1976), BAKER and LAVELLE (1984), GORDON *et al.* (1984) and BISHOP (1986).

The relationship between distributions of suspended particles and c has been examined in several oceanic regions. BISHOP (1986) observed linear relationships between c and the suspended particulate mass in a warm-core ring, the Gulf Stream and the Sargasso Sea. These observations were then used to examine the spatial variability of suspended particles in warm-core ring 82B (BISHOP and JOYCE, 1986). For data collected during the Optical Dynamics Experiment (ODEX) from the R.V. *Acania*, MUELLER *et al.* (1989) found a linear relationship between c from transmissometer measurements and estimates of V using a Coulter counter. They developed linear regressions between c and

* Ocean Physics Group, Department of Geological Sciences, University of Southern California, Los Angeles, CA 90089-0740, U.S.A.
† Present address: Woods Hole Oceanographic Institution, Woods Hole, MA 02543, U.S.A.

V for three depth ranges during ODEX and found that the observed particle size distributions were approximately hyperbolic.

In this paper the relationship between thermohaline water mass variations and c is examined in the neighborhood of the North Pacific Subtropical Front (NPSF). This work follows the preliminary examination of relationships between optical and thermohaline properties by DICKEY *et al.* (1986), which also used a portion of the ODEX data set collected from R.P. *Flip*. Here, variability is examined on time scales from a few hours to 2 weeks and on vertical scales from a few meters to 200 m. Based on the position of the measurement platform over the course of the experiment and a mesoscale CTD/optical survey described by STOCKEL *et al.* (1985), the corresponding horizontal scales range from a few hundred meters up to about 200 km.

One objective of this paper is to characterize values of c for the water masses in the vicinity of the NPSF as has been done previously for temperature, salinity and density (cf. RODEN, 1981; NIILER and REYNOLDS, 1984). The NPSF is a dynamic region with strong geostrophic flows, complex meandering and associated mesoscale eddy activity (VAN WOERT, 1982) that produce lateral mixing and interleaving in the thermohaline fields. These mixing and interleaving processes also should affect the particle fields, and hence the optical properties. This leads to the other objective of this paper which is to examine the effects of isopycnal mixing and advection on the distribution of c in the frontal regions between the large-scale water masses.

The effects of isopycnal mixing and advection on the distribution of c are examined by comparing changes in c along potential density surfaces with corresponding changes in salinity S, which is essentially a conservative tracer here. Isopycnal time series of S and c are computed in the upper 200 m of the water column over a 2 week period and regions of significant correlation are identified. In those regions where changes in c are highly correlated with changes in S, we hypothesize that c behaves as a conservative tracer along isopycnal surfaces. In regions of low or zero correlation, we hypothesize that other processes are more important than isopycnal mixing in controlling the distribution of c. These can include physical, biological and chemical processes such as diapycnal mixing or particle sinking, growth and decay which cause c to be non-conservative along density surfaces. The goal is to differentiate the effects of the basic physical processes of isopycnal mixing and advection from the many other competing effects.

2. EXPERIMENTAL METHOD

Data described in this paper were collected during ODEX from 27 October (JD 300) to 12 November (JD 313) 1982 in the northeast Pacific in the vicinity of 33°N, 142°W. The primary data set used in this paper consists of 255 CTD profiles to a depth of about 200 m obtained from the R.P. *Flip* as it drifted southward across the NPSF. Profiles from JD 300 to 303 were made only to 130 m. The profiling CTD/rosette package carries, among other instruments, a Neil Brown CTD, a Sea Tech beam transmissometer (1 m pathlength, 660 nm wavelength light source; BARTZ *et al.*, 1978) and a SeaMarTech chlorophyll fluorometer. An overview of the R.P. *Flip* component of ODEX which discusses the experimental objectives, instrumentation, and results is given by DICKEY and SIEGEL (1989). The focus here is on the variability of S and c along isopycnal surfaces over 2 weeks of the observational period. Because changes in c along isopycnals are often small, a brief discussion of measurement errors is presented.

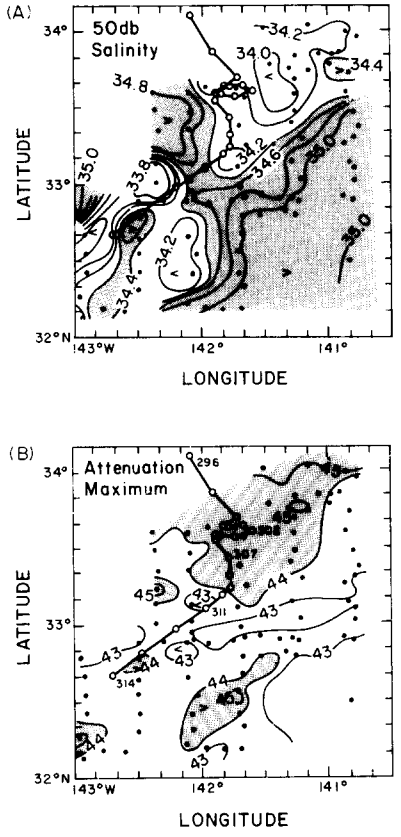

Fig. 1. (A) Salinity on the 50 db surface. Adapted from STOCKEL *et al.* (1986). The track of R.P. *Flip* is shown as a solid line with the position at midnight (GMT) each day indicated by open circles. Stippled areas indicate $S \geq 34.4$. (B) As in (A) but for beam attenuation coefficient c at the depth of the maximum in c. Beam c values are multiplied by 100 and stippled areas indicate $c \geq 0.44$ m^{-1}.

Errors in the absolute value of c are not critical to the results of this paper and are probably small. Measured values of c at the attenuation maximum from the mesoscale survey data of Fig. 1B and from the time-depth contours of Fig. 2B were obtained independently and are in reasonable agreement. Values from both data sets are in the range 0.43–0.44 m^{-1}. Errors in the relative values of c are more important to the results of this paper. The minimum relative error is set by the 16-bit analog-to-digital converter used for acquiring the transmissometer signal; the least count error is about 1.4×10^{-3} % and corresponds to a least count error in c of order 10^{-5} m^{-1}. The contour interval in Fig. 2B and C is 0.0025 m^{-1} or about 0.17% transmission, which is 121 counts of the digitizer. The relative changes in c are typically much larger than this value and are well resolved by the digitizer.

A potentially more troublesome relative error in c can result from the difference in temperature between the transmissometer and the ambient seawater as the instrument is moved vertically through the water column (BISHOP, 1986). One effect of this temperature difference is to produce an offset in c between upcasts and downcasts for a particular station. BISHOP (1986) found that the offset can extend vertically throughout profiles of c.

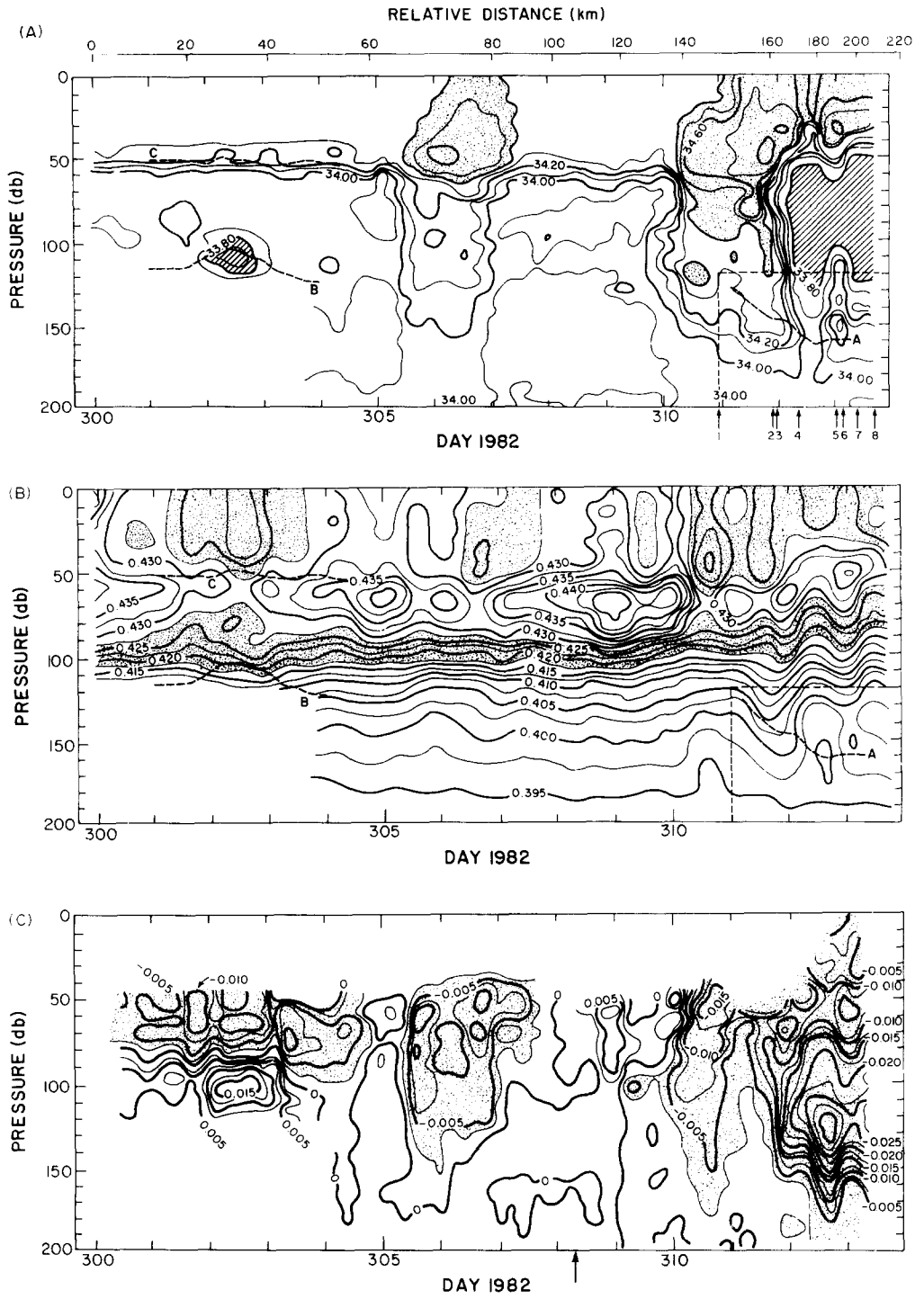
(A)
RELATIVE DISTANCE (km)
0 20 40 60 80 100 120 140 160 180 200 220
PRESSURE (db)
0 50 100 150 200
34.00
34.20
34.60
33.80
C
B
A
300 305 310
DAY 1982
23 4 56 7 8
(B)
0.430
0.435
0.440
0.425
0.420
0.415
0.410
0.405
0.400
0.395
(C)
-0.005
-0.010
0.005
0.015
0.020
0.025
0.010

Fig. 2A–C.

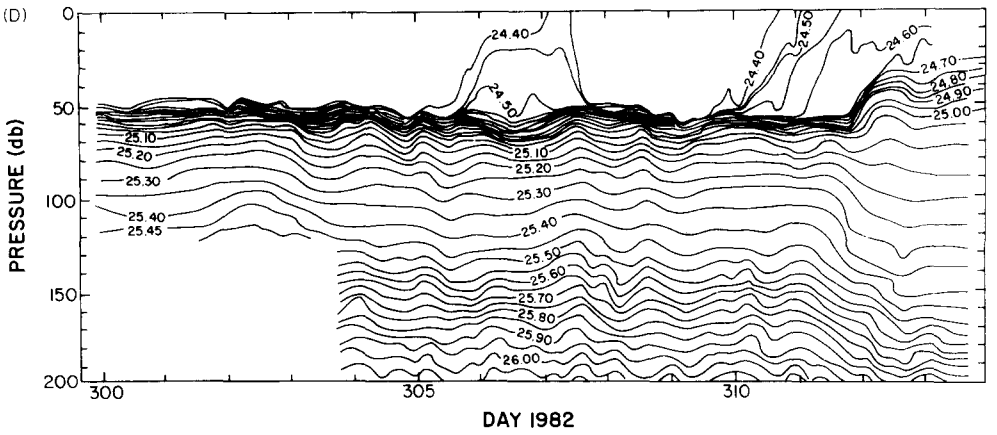

Fig. 2. (A) Time-pressure contours of salinity. Salinities >34.4 are indicated with stippling; those <33.8 with hatching. Profiles of Fig. 3 are contained within the dashed rectangle at lower right. Times of profiles in Fig. 3 are indicated by numbered arrows. Dashed line segments labeled A, B and C indicate positions of isopycnals used in producing scatter plots of Fig. 5. Scale at top gives along-track relative distance starting at day 300. Horizontal scales corresponding to equal time intervals change considerably due to variations in drift speed. (B) As in (A) but for beam attenuation coefficient c. Values for which $0.4225 \leq c \leq 0.4275$ are indicated with stippling. (C) As in (B) but for beam attenuation coefficient anomaly Δc. Values for which $\Delta c \leq 0.0025$ m^{-1} are indicated with stippling. Arrow indicates time of reference profile which is subtracted from each c profile to compute Δc. (D) As in (A) but for σ_θ.

A detailed examination of the transmissometer data showed no evidence of these effects in the present data. This may be due to the fact that the temperature and depth ranges sampled during ODEX were much smaller than those sampled by BISHOP (1986). Relative changes observed in c along isopycnal surfaces are usually seen repeatedly in consecutive profiles, whether upcasts or downcasts.

Occasional spikes may be due to large particles that temporarily block part of the light path of the transmissometer. Very large spikes were edited out of the profiles prior to final processing. Most of the observed spikes are small, however, and can be ignored; their effect on the results and conclusions are negligible. Two examples of these spikes can be seen in the vertical c profiles of Fig. 3: one at 178 db (panel 3) and another at 141 db (panel 6).

3. MESOSCALE VARIABILITY AND TIME SERIES DURING ODEX

An association between mesoscale thermohaline and optical property distributions is indicated in the horizontal section of S at 50 db and c at the depth of the beam attenuation maximum (Fig. 1A and B; adapted from STOCKEL *et al.*, 1986). A mesoscale map of the depth of the attenuation maximum, given by STOCKEL *et al.* (1986), shows that this maximum occurs between 50 and 70 m, so the maps of Fig. 1A and B are comparable. This depth range is in agreement with the pressure range corresponding to the maximum in c of Fig. 2B.

It is apparent from Fig. 1A and B that the low salinity water mass ($S \leq 34.4$) in the northeast quadrant also has higher values of c at the beam attenuation maximum, with $c \geq 0.44$ m^{-1}. This maximum typically occurs just below the surface mixed layer in the

region (PAK *et al.*, 1988; DICKEY and SIEGEL, 1989). Further to the southwest along the track of R.P. *Flip* (Fig. 1A, B), salinity increases to a maximum while c decreases to a minimum at the position occupied by R.P. *Flip* on day 311. For the remainder of the track, salinity is variable at 50 db, but typically less than about 34.4, and values of c are generally lower than 0.44 m^{-1}.

High surface salinities are first encountered from R.P. *Flip* on days 306 and 307 and then from day 311 until the end of the experiment (Fig. 2A). The similar T–S characteristics [see DICKEY and SIEGEL (1989) for the temperature time series] during these two time intervals indicate that the same water mass has been encountered. This high salinity water mass is the same as that in the mesoscale survey of Fig. 1A. Time series of S and c which would be inferred from Fig. 1A and B along the track are in reasonable agreement with properties measured from R.P. *Flip*, although the station spacing of the mesoscale survey is quite coarse. In the northeast Pacific, the NPSF is identified by a near-surface, horizontal salinity gradient; at 137°W this gradient occurs for 100 m salinities in the range 34.2–34.8 (NIILER and REYNOLDS, 1984). Horizontal salinity gradients at 100 m in this salinity range are found for these data (Fig. 2A).

A correspondence between the high salinity waters above 60 db and low values of c may easily be seen on days 306 and 307 and from day 310 until the end of the experiment (Fig. 2A, B). These high salinity, near-surface waters also have reduced attenuation maxima which is in agreement with the mesoscale date of Fig. 1. A water mass with low c, but without accompanying thermohaline variations is also found in the surface layer on days 301 and 302. The depth-time contours above 130 m from day 300 to 304, which includes this time period, are nearly symmetric and appear "folded" about day 302.5. Such a pattern can be accounted for by the motion of R.P. *Flip* as it moved in an elongated loop over this time interval. Careful examination of a detailed plot (not shown) of the drift track of R.P. *Flip* shows that the easternmost point of the loop was reached on day 302.5. The observed sequence is consistent with motion first into and then out of a water mass having horizontally uniform salinity (in the surface layer), but with lower values of c. Chlorophyll fluorescence also decreased in a similar manner in this water mass (DICKEY and SIEGEL, 1989).

An interesting feature of the near-surface c time series is a diurnal cycle with an amplitude of about 0.006 m^{-1}. This is particularly evident in Fig. 2B beginning on day 305 above 50 db and somewhat obscures longer temporal scale variability associated with thermohaline changes. SIEGEL *et al.* (1989) discuss this diurnal periodicity in detail and show it to be significant to a depth of 95 m, the depth of the euphotic zone. They also have developed a simple biological model of particulate growth (related to photosynthesis) and removal (by grazing) that accounts for the periodicity.

A correspondence between thermohaline variations and c is also found deeper in the time series, but is not as apparent as that near the surface. A 50 db upward displacement of the 0.3975 m^{-1} contour on day 312 (Fig. 2B), which indicates a water mass with lower particle concentrations, coincides with an interleaving of fresher water in the same depth range (Fig. 2A). In contrast to the negative correlations observed near the surface, changes in S and c are positively correlated in this time-pressure range. The difficulty in identifying variability in c associated with thermohaline water mass differences below the surface layer is due to the strong trend of decreasing c with depth found in all profiles. This trend is found everywhere below about 60 db (Fig. 2B) and is likely caused by the combined effects of particulate production, aggregation, sinking and vertical mixing (cf.

JERLOV, 1976; PARSONS *et al.*, 1984). To examine variations in c deeper in the water column, an anomaly is defined which effectively removes this trend.

The anomaly Δc is formed by subtracting a reference profile from each measured c profile at specified levels of σ_θ. Values of Δc are computed at σ_θ intervals of $\Delta\sigma_\theta = 0.005$ kg m^{-3}. We used a single profile on day 308.3 to be the reference. This profile was chosen to differentiate between the high salinity water mass, found from day 305 to 307 and at the end of the experiment, and the low salinity water mass encountered between these times. Thermohaline characteristics of this reference profile are consistent with North Pacific Intermediate Water (RODEN, 1975; NIILER and REYNOLDS, 1984; DICKEY and SIEGEL, 1989). However, the results of the anomaly analysis are not critically dependent on the choice of reference profile.

A clear correspondence between Δc and S over much of the water column is now evident. The high salinity water encountered between days 305 and 307 and between 310 and 312 is also relatively clear; high salinity and low Δc are coincident to pressures of about 175 db (Fig. 2C). This decrease in c below the surface layer is barely discernible in Fig. 2B, particularly on days 305–307. A maximum in Δc ($\Delta c \geq 0.015$ m^{-1}) is associated with the local minimum in salinity found on day 302 at 110 db. This is in contrast to the lower Δc ($-0.020 \leq \Delta c \leq -0.100$ m^{-1}) associated with the other low salinity water mass beginning on day 312 between 50 and 120 db. Data are generally absent in the surface layer because of the small density differences found there and the fact that density surfaces outcrop (Fig. 2D).

The positive correlation between S and c (for $p \leq 120$ db) after day 310 (Fig. 2A, B) is also clearly seen in the vertical finestructure of these properties (Fig. 3). In representative background profiles, small local maxima in both S and c are found at 180 db (panel 1). Later, large maxima in both S and c have intruded higher into the water column, with an anomaly in S of about 0.14 and in c of about 0.005 m^{-1} (panels 3 and 4). The thickness of this intruding water mass is about 30 m, assuming 1 db = 1 m. These maxima are made more evident in the profiles by the intrusion of a thinner, but fresher and lower c, water mass centered at about 134 db (panel 2) and 150 db (panel 3). The change in depth of the maxima is about the same as the change in depth of the $\sigma_\theta = 25.45$ surface and indicates that the intrusion is oriented along sloping density surfaces. Small-scale irregularities in the S and c profiles suggest interleaving on vertical scales of 2–4 m at the depth of the maxima.

After 10 h, the maxima are absent from the profiles and have been replaced by a fresher, less turbid water mass (panel 4). However, the maxima are found again later in about the same depth range (panels 5 and 6). These alternate encounters with saline, turbid waters and relatively fresh, clear waters suggest interleaving on horizontal scales of order 20 km based on the drift of R.P. *Flip* (Fig. 2). A thin layer of lower c and relatively fresh water lies just above the maxima (panels 6 and 7) and is similar to that found earlier at the same depths (panels 3 and 4). The intrusion is slightly higher in the water column (panel 6) while later the maxima have decreased in vertical extent (panel 7). A second pair of maxima in S and c are also found just below the 25.45 isopycnal (panel 7). After about 8 h, a single pair of maxima are again found (panel 8) and the intrusion is found at its greatest depth, about 170 db.

The trend of the 25.45 isopycnal to generally deepen as the experiment progressed (Fig. 3) is found for all isopycnals below 100 m beginning on day 311 (Fig. 2D). It is also apparent that the warmer, high salinity water found in the surface layer is also of higher

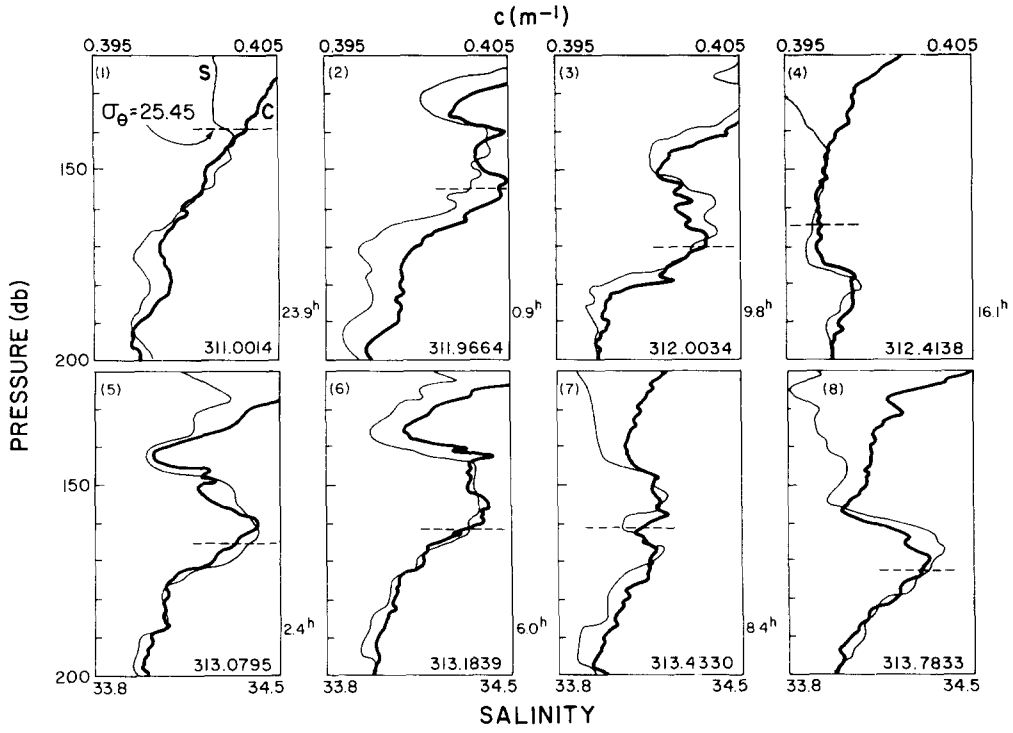

Fig. 3. Sequence of vertical profiles of S (thin line) and c (bold line). Time in days is given at lower right of each panel and time interval in hours between profiles is given between panels. Numbers at upper left of each panel correspond to arrows along time axis in Fig. 2A. Depth-pressure range of these profiles is indicated by dashed rectangles at lower right corners of Fig. 2A and B. Position of σ_θ 25.45 isopycnal is indicated by dashed line segments.

density. However, below the mixed layer before day 311, thermal fronts are nearly compensated in density by increased salinity. The salinity compensation of thermal fronts has been previously observed for the NPSF (RODEN, 1975; NIILER and REYNOLDS, 1984). Beginning on day 312, when the low salinity water is encountered between 50 and 120 db, the depth between isopycnal surfaces increases, resulting in a weaker seasonal thermocline at about 40 db and a less stable water column down to about 150 db. Other aspects of the thermohaline variability and its influence upon bio-optical distributions are discussed by DICKEY and SIEGEL (1989).

4. ISOPYCNAL VARIABILITY OF SALINITY AND BEAM ATTENUATION

In order to examine more objectively the distributions and correlations between changes in S and c, time series were formed by interpolating data points both onto equal time intervals of 0.1 days and onto isopycnal surfaces. These time series were computed for all isopycnal surfaces between 0 and 200 db with a spacing of $\Delta\sigma_\theta = 0.05$ kg m^{-3}, as shown in Fig. 2D.

These time series show that changes in S and c are often highly correlated below the 1% light level. For example, on the 25.45 isopycnal S and c are generally negatively

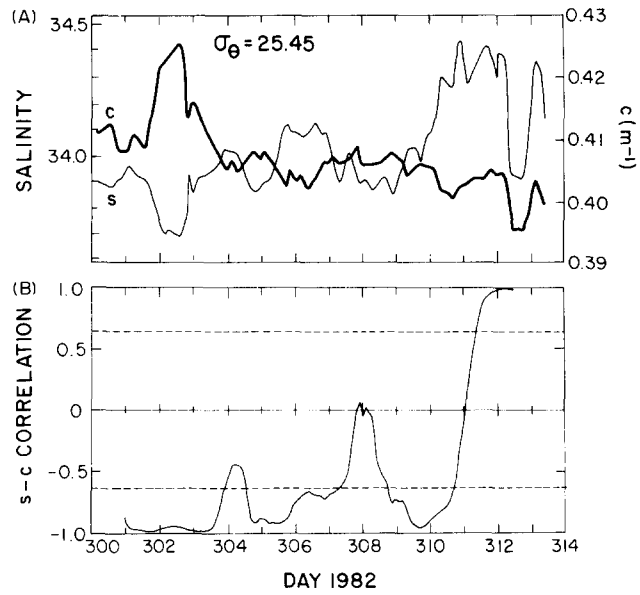

Fig. 4. (A) Time series of S (thin line) and c (bold line) on σ_θ = 25.45 isopycnal. (B) Time series of 2 day correlation coefficient between S and c on the σ_θ = 25.45 isopycnal. Dashed lines indicate 95% confidence limits for non-zero correlation.

correlated (Fig. 4A): as S decreases by 0.25 between days 302 and 303, c increases by 0.02 m^{-1}. The pressure of the 25.45 surface increases during the time of these observations from 115 db on day 300 to 170 db on day 313 (Fig. 2D). This pressure range exceeds the depth of the 1% light level (95 m, SIEGEL and DICKEY, 1987) throughout the time period and diurnal variations in c are absent. Much smaller decreases in c are associated with increases in S on days 305–306 and days 310–311. In contrast, S and c are positively correlated during the last 24 h period of the time series (Fig. 3). Not all changes in thermohaline properties are accompanied by changes in c, however. From day 310.5 to 311.7, for example, small-scale interleaving in S (and T) is found with little change in c.

The apparent visual correlation evident in sections of the time series in Fig. 4A is better seen in scatter plots of c vs S. Along segments of many isopycnal surfaces, points scatter along lines between pairs of end members. In an example of positive correlation (Fig. 5A), one end member is the high salinity water found toward either end of a segment of the 25.45 isopycnal (dashed line A, Fig. 2A,B) while the other is the low salinity water mass about half way along the segment. This latter, interleaving water mass is also less turbid and gives rise to the positive S–c correlation. Water of intermediate properties is consistent with local isopycnal mixing between these end members.

A contrasting example of negative correlation (Fig. 5B) is also found on a segment of the 25.45 isopycnal from day 301 to day 304 (dashed line B, Fig. 2A,B). In this case the low salinity water is more turbid and results in the negative S–c correlation. Changes in S and c are frequently uncorrelated along isopycnals. An example of essentially zero correlation is found along the shallow 24.50 isopycnal from days 301 to 304.3 (Fig. 5C). Here, isopycnal salinity gradients are low while those in c are large. Because of this,

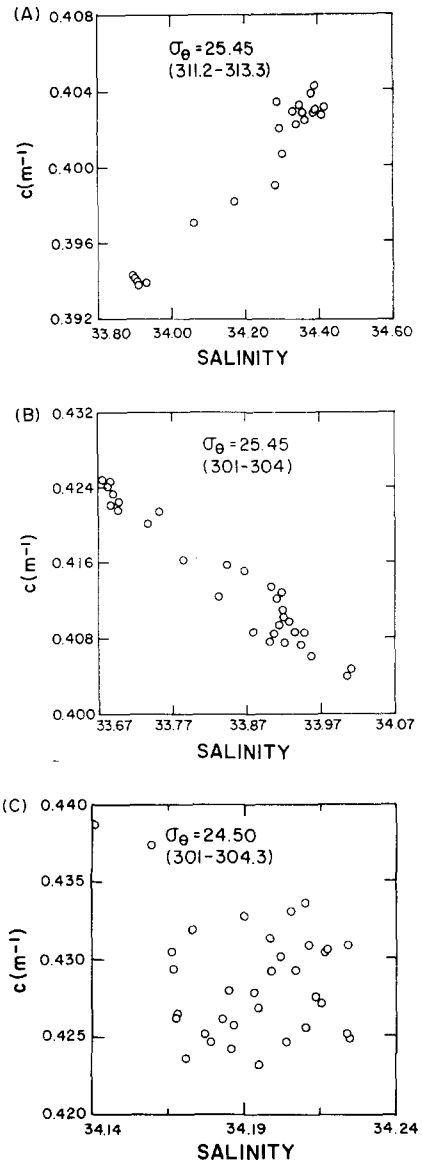

Fig. 5. (A) Scatter plot of c vs S on $\sigma_\theta = 25.45$ isopycnal from day 311.2 to 313.3. Depths of $\sigma_\theta = 24.45$ during this time period are indicated in Fig. 2A and B with dashed line labeled A. (B) As in (A) but for days 301–304. Depths of $\sigma_\theta = 25.45$ during this time period are indicated in Fig. 2A and B with dashed line labeled B. (C) As in (A) but for days 301–304 on $\sigma_\theta = 24.50$. Depths of $\sigma_\theta = 25.50$ during this time period are indicated in Fig. 2A and B with dashed line labeled C.

mixing processes can produce large changes in c with little corresponding change in S. Furthermore, this isopycnal is found at the base of the mixed layer, well within the euphotic zone, where diurnal changes in c are large.

To examine the relationship between c and S more systematically for the entire data set, a 2 day moving correlation function r was computed between S and c along isopycnal

surfaces in the upper 200 m of the water column. The 2 day window is a compromise between resolving shorter time scale correlations and acquiring sufficient degrees of freedom to produce statistically significant estimates of r. The number of profiles obtained for each 2 day period during this part of ODEX varied from a minimum of 10 to a maximum of more than 40 during periods when the instrument package was continuously raised and lowered between the surface and 200 m (DICKEY *et al.*, 1986; DICKEY and SIEGEL, 1989). The number of degrees of freedom for computing r is conservatively estimated to be 10, consistent with the lowest sampling rate.

The time series of r for the $\sigma_\theta = 25.45$ surface shows that water mass boundary crossings are generally accompanied by absolute values of $r > 0.80$ (Fig. 4B). The correlation between changes in S and c on the $\sigma_\theta = 25.45$ isopycnal are significantly non-zero more than 70% of the time over the 11.5 day period for which r is defined. Extensive regions of high S–c correlation are found throughout much of the time-depth range of the experiment (Fig. 6). The negative correlation observed on the 25.45 surface is seen to be part of a large region of high S–c correlation extending vertically from 60 to 170 db for the final 2 days of the experiment. A transition in the water column is suggested at the depth of the 1% light level: strong correlation is encountered more frequently in the 50 db immediately below the 1% light level compared with the 50 db above. Correlations below 150 db are generally low because isopycnal gradients are weak and mixing and advection produce little change in S and c.

Changes in S and c are highly correlated ($|r| \geq 0.8$) for more than 30% of the observation time for a narrow range of isopycnals centered on σ_θ 25.4 kg m^{-3} (Fig. 7A). This potential density range corresponds to about 40 m of the water column and lies just below the 1% light level (Fig. 7B). Isopycnal surfaces lying above the 24.95 surface also exhibit high S–c correlations for more than 30% of the observation time. The generally small difference between profiles of $r \leq -0.8$ and $|r| \geq 0.8$ indicates that negative S–c

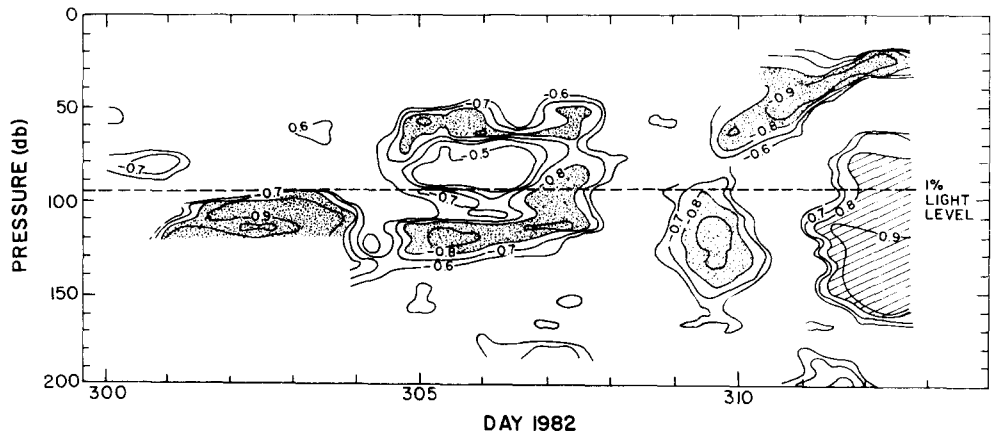

Fig. 6. Time-pressure contour plot of 2 day correlation coefficient between S and c. Correlation coefficient is computed along isopycnal surfaces separated by $\sigma_\theta = 0.05$ kg m^{-3}. Regions for which $r \leq 0.80$ are stippled; those for which $r \geq 0.80$ are hatched. Only contours for which the correlation function is significantly non-zero at a 95% confidence level are shown. Dashed line indicates depth of the 1% light level (95 m). Most of the surface layer is excluded from the contour plot because of outcropping of isopycnals. The $\sigma_\theta = 24.50$ surface was the most shallow isopycnal used in computing r.

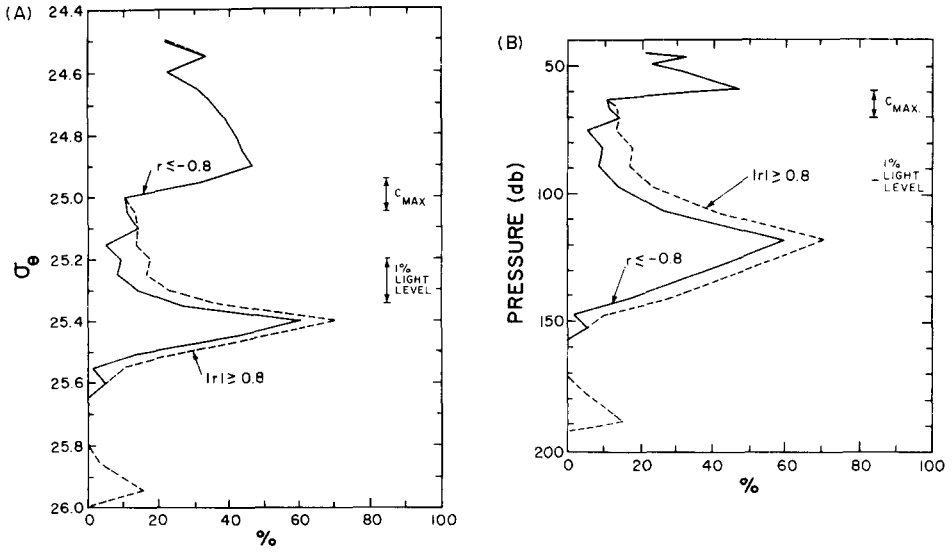

Fig. 7. (A) Fraction of observation time vs σ_θ for which $|r| \geq 0.8$ (dashed line) and $r \leq 0.80$ (solid line) where r is the correlation coefficient between S and c. (B) As in (A) but vs pressure.

correlations are most frequently observed along a given isopycnal. An abrupt drop in the frequency of high S–c correlation is found at the level of the maximum in c. The frequency of high correlation remains low, with $|r| \geq 0.8$ for generally less than 15% of the record, until the depth of the 1% light level is exceeded.

5. DISCUSSION AND CONCLUSIONS

Time series of salinity S and the beam attenuation coefficient c indicate a complex meandering frontal structure in the vicinity of the NPSF. Within the surface mixed layer, observed salinities toward the southern side of the NPSF are in the range 34.4–34.8 and c is generally <0.4275 m^{-1}, similar to properties of the North Pacific Subtropical Water mass (RODEN, 1975; DICKEY and SIEGEL, 1989). Toward the northern side of the NPSF, salinities are lower (<34.4), while c is higher (in the range 0.4275–0.4350). DICKEY and SIEGEL (1989) have shown that this is consistent with North Pacific Intermediate Water. The surface S distribution is qualitatively similar to that observed by RODEN (1981) in the region near 30°N, 153°W. An anomaly in the beam attenuation coefficient is defined on density surfaces and shows that the correspondence between distributions of S and c extends to a depth of about 200 m.

Changes in S and c along isopycnal surfaces are often correlated on a 2 day time scale with c–S points scattering along mixing lines between pairs of end members. We interpret these temporal correlations to reflect spatial correlations between the S and c fields on horizontal scales of order 10–30 km. The observed correlations are consistent with the hypothesis that isopycnal mixing and advection are important in controlling particle concentrations and hence c. Horizontal shearing and advective processes, which are active in frontal regions like the NPSF, drive mesoscale eddies and isopycnal mixing processes. These result in the formation of many smaller scale water parcels with S–c

properties intermediate between those of the large-scale water masses from which they are derived. Other processes which tend to reduce correlation between changes in S and c are also active and obscure variability due to isopycnal physical processes. One of these is diurnal variability in c which is observed above the 1% light level in the euphotic zone. These observations suggest that the 1% light level may represent a transition depth. Above this level, non-conservative processes like particle sources and sinks appear to dominate changes in c, while isopycnal mixing and advection are important below.

The frequency of high S–c correlation along isopycnals is probably underestimated for two reasons. First, the correlation between S and c can only be observed in regions where strong local isopycnal gradients are found in both quantities, regardless of the intensity of mixing. Second, it is possible that more than two water masses with characteristic S and c values may be mixing together over 10–30 km horizontal scales (or over any other spatial scale chosen for computing r). Even in the absence of other processes, simultaneous mixing among three or more water masses with differing end members could result in a scatter plot similar to that in Fig. 5C for which r is essentially zero.

The horizontal scale of the mixing and advection processes may be crudely estimated from the isopycnal changes in S or c and the magnitudes of the isopycnal gradients. The horizontal gradient in S for the time period of Fig. 5A is approximately $\Delta S/\Delta x \sim 0.03$ km^{-1}. The maximum change in S in Fig. 5A is about $\Delta S \sim 0.4$ which indicates an eddy mixing length of order $\Delta l \sim \Delta S/(\Delta S/\Delta x) \sim 13$ km. Vertical movement of particles and optical properties may also result from motion along isopycnals because these surfaces slope due to the geostrophic velocity field. Average slopes below 100 m are of order 10^{-3} over the last 4 days of the experiment. A 13 km eddy could, therefore, produce a vertical movement of order $\Delta z \sim 13$ m which is comparable to the depth changes of fine structure features of c shown in Fig. 3.

These observations indicate that isopycnal mixing and advection processes are important in redistributing particles both horizontally and vertically in the vicinity of the NPSF. Models of particle dynamics in open ocean frontal regions must, therefore, account for these advective and mixing effects. The degree to which c behaves as a conservative tracer is still an open question, although much of the observed variance in c on spatial scales of order 10–30 km is consistent with this behavior, particularly below the 1% light level.

Acknowledgements—Discussions with James Mueller during this work were most helpful. This research was supported by the Ocean Optics Program of the Office of Naval Research under contract N00014-87-K-0138.

REFERENCES

BAKER E. T. and J. W. LAVELLE (1984) The effect of particle size on the light attenuation coefficient of natural suspensions. *Journal of Geophysical Research*, **89**, 8197–8204.

BARTZ R., J. R. V. ZANEVELD and H. PAK (1978) A transmissometer for profiling and moored observations in water. *Proceedings of the Society of Photo-Optical Instrumentation Engineers (Ocean Optics V)*, **160**, 102–108.

BISHOP J. K. B. (1986) The correction and suspended particulate matter calibration of Sea Tech tranmissometer data. *Deep-Sea Research*, **33**, 121–134.

BISHOP J. K. B. and T. M. JOYCE (1986) Spatial distributions and variability of suspended particulate matter in warm-core ring 82B. *Deep-Sea Research*, **33**, 1741–1760.

DICKEY T. D. and D. A. SIEGEL (1989) Physical, chemical, bio-optical, and meteorological variability in the eastern North Pacific Ocean. Unpublished manuscript.

DICKEY T. D., D. A. SIEGEL, A. BRATKOVICH and L. WASHBURN (1986) Optical features associated with thermohaline structures. *Proceedings of the Society of Photo-Optical Instrumentation Engineers* (*Ocean Optics* VIII), **637**, 308–313.

GORDON J. R., R. C. SMITH and J. R. V. ZANEVELD (1984) Introduction to ocean optics. *Proceedings of the Society of Photo-Optical Instrumentation Engineers* (*Ocean Optics* VII), **489**, 2–41.

JERLOV N. G. (1976) *Marine optics*, Elsevier, New York, 231 pp.

MELLER J. L., H. PALE, R. C. SMITH, J. R. V. ZANEVELD, R. W. AUSTIN, D. A. KIEFER, B. G. MITCHELL, J. C. KITCHEN and K. S. BAKER (1989) Bio-optical and physical spatial variability in the eastern North Pacific in October–November, 1982. Unpublished manuscript.

NIILER P. P. and R. W. REYNOLDS (1984) The three-dimensional circulation near the eastern North Pacific Subtropical Front. *Journal of Physical Oceanography*, **14**, 217–230.

PAK H., D. A. KIEFER and J. C. KITCHEN (1988) Meridional variations in the concentration of chlorophyll and microparticles in the North Pacific Ocean. *Deep-Sea Research*, **35**, 1151–1171.

PARSONS T. R., M. TAKAHASHI and B. HARGRAVE (1984) *Biological Oceanographic Processes*, 3rd edn, Pergamon Press, Oxford, 330 pp.

RODEN G. (1975) On North Pacific temperature, salinity, sound velocity and density fronts and their relation to the wind and energy fluxes. *Journal of Physical Oceanography*, **15**, 557–571.

RODEN G. (1981) Mesoscale thermohaline, sound velocity, and baroclinic flow structure of the Pacific Subtropical Front during the winter of 1980. *Journal of Physical Oceanography*, **11**, 658–675.

SIEGEL D. A. and T. D. DICKEY (1987) On the parameterization of irradiance for open ocean photoprocesses. *Journal of Geophysical Research*, **92**, 14,648–14,662.

SIEGEL D. A., T. D. DICKEY, L. WASHBURN, M. K. HAMILTON and B. G. MITCHELL (1989) Optical determination of particulate abundance and production variations in the oligotrophic ocean. *Deep-Sea Research*, **36**, 211–222.

SPINRAD R. W. (1986) A calibration diagram of specific beam attenuation. *Journal of Geophysical Research*, **91**, 7761–7764.

STOCKEL J. A., J. L. MUELLER, H. PAK and D. MENZIES (1986) Data from the Optical Dynamics Experiment (ODEX) R/V *Acania* expedition of 10 Oct. thru 17 Nov. 1982 Volume 1: CTD and optical profiles. Data Report NPS-68-86-013, Naval Postgraduate School, Monterey, California.

VAN WOERT M. (1982) The subtropical front: Satellite observations during FRONTS 80. *Journal of Geophysical Research*, **87**, 9523–9536.